ELSEVIER

Contents lists available at ScienceDirect

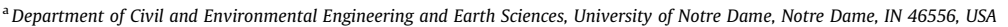
Geochimica et Cosmochimica Acta

journal homepage: www.elsevier.com/locate/gca



Reduction of selenite by bacterial exudates

Leah C. Sullivan ^{a,*}, Maxim I. Boyanov ^{b,c}, Joshua T. Wright ^d, Mark C. Warren ^d, Kenneth M. Kemner ^c, Jeremy B. Fein ^a



^b Bulgarian Academy of Sciences, Institute of Chemical Engineering, Sofia 1113, Bulgaria

ARTICLE INFO

Article history: Received 8 September 2022 Accepted 6 October 2022 Available online 13 October 2022 Associate editor: Colleen M. Hansel

Keywords: Selenite reduction Bacterial exudates Sulfhydryl sites

ABSTRACT

Bacterial reduction of Se(IV) is a significant component of the global selenium cycle, and hence affects the fate and transport of selenium in both natural and contaminated environments. However, it is unknown whether bacterially-produced exudates are capable of reducing selenium independent of bacterial cells. In this study, we measured the rate and extent of Se(IV) reduction by exudates from three bacterial species, and we determined the importance of exudate sulfhydryl sites by conducting parallel experiments after treatment of the exudates with a sulfhydryl-specific blocking molecule. We also conducted experiments with whole cell biomass for each of the three bacterial species to determine the importance of exudate-only reduction relative to whole biomass-promoted reduction. Under our experimental conditions, exudates from Bacillus subtilis and Pseudomonas putida remove Se(IV) from solution after an approximately 20-24 h lag period, but exudates from Shewanella oneidensis are ineffective at Se(IV) removal, except when the cells are grown in the presence of Se(IV). For both B. subtilis and P. putida, pretreatment blocking of the sulfhydryl sites on the exudate molecules dramatically decreases the rate and extent of Se (IV) removal, strongly suggesting that sulfhydryl groups on the exudate molecules play a key role in the Se(IV) reduction mechanism. The behavior of S. oneidensis exudates indicates that up-regulation of the Se (IV) reduction mechanism can occur in response to the Se content of the medium in which the cells grow. Our results demonstrate the capacity of some bacterial exudates to reduce Se(IV), and suggest that the activity of bacterial exudates should be accounted for when modeling selenium cycling in natural and engineered environments.

© 2022 Published by Elsevier Ltd.

1. Introduction

The reactions that control the speciation and fate of selenium in soil and groundwater systems are typically controlled by bacteria, and a wide range of bacterial species are capable of promoting selenium reduction or oxidation reactions (Garbisu et al., 1996; Stolz et al., 2006; Winkel et al., 2012; Vogel et al., 2018). The environmental behavior of selenium is controlled by its redox chemistry, with the dominant forms being selenate (Se[VI]) and selenite (Se[IV]) which are present in surface and groundwaters as highly mobile anionic species (Robberecht and Van Grieken, 1982). In addition, elemental Se(0), which is relatively insoluble but can be present as potentially mobile nanoparticles, and sele-

E-mail address: lsulli10@nd.edu (L.C. Sullivan).

nide (Se[-II]) which exhibits similar geochemistry to sulfide and is relatively insoluble, become important components of the selenium cycle under reducing conditions, while organic selenium compounds may be found as soluble or volatile species (Masscheleyn et al., 1990). Understanding the controls on selenium biogeochemistry is critical not only for understanding the global cycling and environmental behavior of selenium, but also for designing effective remediation approaches for Se-contaminated waters.

Anaerobic respiration reductases in the bacterial cell periplasmic space serve as the terminal selenite reductases during bacterial reduction of Se(IV) to Se(0) (Li et al., 2014). Because the site for selenite reduction by bacteria is located in the periplasmic space of the cell envelope, the first step in reduction must be the binding of aqueous selenite to the cell surface. Under circumneutral pH conditions, bacterial cell surfaces are strongly negatively charged; however, the electrostatic repulsion between the cell surface and aqueous anionic selenite can be overcome by binding of



^c Biosciences Division, Argonne National Laboratory, IL 60439, USA

^d Department of Physics, Illinois Institute of Technology, Chicago, IL 60616, USA

^{*} Corresponding author at: Department of Civil and Environmental Engineering and Earth Sciences, University of Notre Dame, 156 Fitzpatrick Hall, Notre Dame, IN 46556 USA.

selenite onto cell surface sulfhydryl sites (Yu et al., 2018). The concentration of these sulfhydryl sites and their distribution between the cell surface and bound extracellular polymeric substances (EPS) molecules varies widely between bacterial species. Some bacteria, such as *Shewanella oneidensis*, have the vast majority of their surface sulfhydryl sites located on the cell surface; other species like *Pseudomonas putida* have sulfhydryl binding sites located primarily on exuded EPS molecules that are tightly bound to the cell surface; and other species like *Bacillus subtilis* have a more even distribution between the two extremes (Yu and Fein, 2016).

Soluble organic molecules that are exuded by bacteria can reduce aqueous Au(III), and they contain a range of proton-active functional groups (Kenney and Fein, 2011a; Seders and Fein, 2011), possibly including sulfhydryl sites (Kenney and Fein, 2011a; Yu and Fein, 2016). Hence, bacterial exudates may promote selenite reduction in much the same way that occurs at the cell surface. The objective of this study was to isolate seleniteexudate interactions to determine whether bacterial exudates can cause significant reduction of aqueous selenite, and to determine whether exudate-bound sulfhydryl sites play a role in selenite reduction. Similar to the differences between bacterial species in the location and concentration of sulfhydryl sites on their EPS molecules, the ability of bacterial exudates to reduce selenite may vary significantly between species. Therefore, we tested exudates from three different common species of bacteria, B. subtilis, P. putida, and S. oneidensis, because of the range of sulfhydryl site concentrations on the exudate molecules from these species. Furthermore, we compared exudate-promoted selenite reduction rates to the rate of selenite reduction by bacterial cells to quantify the relative importance of bacterial exudates in the bioreduction of selenite. In addition, we used X-ray absorption spectroscopy (XAS) to characterize the valence state and binding environment of Se in the exudate solutions under the experimental conditions. The results of this study improve our understanding environmentally-relevant bioreduction pathways for selenite, and thereby could be used to optimize bioremediation strategies for selenite-contaminated waters.

2. Methods

2.1. Bacterial growth and preparation of exudate solutions

Exudates were prepared from pure cultures of B. subtilis, P. putida, and S. oneidensis to examine bacterial exudates that contain a range of concentrations of sulfhydryl sites. Bacterial cells were cultured aerobically in 3 mL of trypticase soy broth (TSB, BD Difco) at 30C for 24 h, then transferred to 2 L of TSB with 50 g/L of glucose added and incubated aerobically with gentle agitation for an additional 24 h at 30°C. Bacterial biomass was harvested by centrifugation at 8500 g for 5 min. This was followed by three rinse steps, which consisted of suspending the bacterial pellet in a fresh 0.01 M NaCl solution and centrifuging at 8500 g for 5 min, to remove any remaining culture medium from the biomass. After the third rinse, the supernatant was then poured off and each pellet was transferred to a pre-weighed centrifuge tube. Each pellet was then centrifuged twice at 8500 g for 30 min, removing the supernatant both times, after which the mass of the pellet was recorded. The biomass was resuspended in 0.01 M NaCl at a concentration of either 20 or 50 g biomass per 1 L of 0.01 M NaCl solution to produce the exudate solution. Initially, all exudate solutions were produced at a concentration of 20 g of biomass/L. At this initial concentration, we observed no reduction in the S. oneidensis experiments, hence we increased to 50 g/L the S. oneidensis concentrations used to produce the exudates to determine if higher exudate concentrations would promote reduction. In each case, the cell suspension was kept at room temperature for 72 h on an orbital shaker operating at 100 rpm to allow the bacteria to exude a range of organic molecules. Previous FTIR studies of these exudates indicate the presence of polysaccharides, and amide I and amide II peaks (Seders and Fein, 2011). After the 72 h soak, the biomass was separated from the soluble exudates by centrifugation at 8500 g for 5 min to pellet the majority of the biomass. The supernatant was then filtered through a 0.45 µm cellulose acetate membrane (Corning) to create the exudate-bearing solution that was used in the Types 1 and 2 sets of experiments (described below). We use the term 'exudates' to refer to the soluble organic components released from the bacterial biomass, either through active production or as a consequence of cell lysis; by this definition, the exudates are physically distinct from what we refer to as EPS which are cell-bound actively-produced insoluble molecules.

2.2. Selenite reduction experiments

We conducted selenite reduction experiments to determine the role of sulfhydryl sites and the relative importance of exudates and whole cells in selenite reduction. Five types of experiments were conducted: Type 1- involving untreated bacterial exudates, Type 2 – involving exudates that had been treated with a sulfhydryl site blocking agent, Type 3 – involving untreated whole-cell biomass, in which the bacterial cells were not separated from the exudates, Type 4 – involving whole cell biomass that was treated with the sulfhydryl site blocking agent, and Type 5 – involving exudates from *S. oneidensis* cells that were cultured in the presence of Se (IV) in the growth medium.

The Type 1 experiments involved the exudate-bearing solutions directly without further treatment. To each solution, selenite was added to achieve an initial concentration of ~ 10 ppm, using 10 mL/L of a 1000 ppm stock solution of sodium selenite dissolved in 0.01 M NaCl. After the Se addition, samples were taken every 24 h from 0 h to 96 h to test for Se removal from solution; For this, a portion of the exudate solution was removed and centrifuged at 12,000 g for 5 min followed by the removal of the supernatant, avoiding disruption of any pellet that was formed. The supernatant was then acidified to prevent further reaction and stored for ICP analysis. Experiments were conducted in triplicate.

The Type 2 experiments were conducted to assess if exudatebound sulfhydryl binding sites control selenite reduction by the bacterial exudates. These experiments were identical to the Type 1 experiments, except that prior to use in the experiments the exudate solution was treated with monobromo(trimethylammonio)b imane bromide (qBBr, Toronto Research Chemicals, Toronto, Ontario, Canada), a molecule that reacts specifically and irreversibly to block sulfhydryl sites from further reactivity (Joe-Wong et al., 2012; Yu et al., 2014), at a concentration of 36 µmol/gram of biomass used to make the exudate solution. We do not know the exact sulfhydryl site concentration of the exudate solution, but estimating an average sulfhydryl concentration of 30 µmol/g biomass/L as one-third of the total expected protonactive sites (Yu et al., 2014), the qBBr concentration was approximately 1.2 times the expected sulfhydryl concentration to ensure complete blocking of the sulfhydryl sites on the exudates from each of the bacterial species. After a 2 h reaction period between the qBBr and the exudate, which has been shown previously to be sufficient to allow complete reaction between sulfhydryl sites and qBBr (Yu and Fein, 2017), selenite was added, and sampling was conducted as described above.

For the Type 3 whole-cell biomass experiments, the cell preparation procedure was the same as that used to produce the exudate-bearing solutions up to the 72 h incubation period and subsequent filtration. After the mass of the bacterial pellet was determined, however, instead of being discarded, the bacterial pel-

let was resuspended in a fresh 0.01 M NaCl solution to achieve a cell suspension concentration of 20 g wet biomass/L, selenite was added, and samples were extracted as described above.

The preparation procedure for the Type 4 whole-cell experiments involving biomass treated with qBBr was the same as that described above for the Type 3 whole-cell experiments until the resuspension step, at which point qBBr was added to the 20 g wet biomass/L bacterial suspension in 0.01 M NaCl at a concentration of 180 µmol/g of biomass and allowed to react with the biomass for 2 h. This concentration has been previously determined to be in an approximate 2:1 stoichiometric ratio of qBBr: bacterial sulfhydryl sites for the bacterial species used here and allows for saturation of these sites by the qBBr (Yu et al., 2018). Two variations of these Type 4 whole-cell qBBr-exposure experiments were conducted: 1) those with excess qBBr present even after the addition of Se to block sulfhydryl sites on the cell surfaces as well as on the exudates from the cells that are released during the course of the experiments; and 2) those in which excess qBBr is removed prior to the addition of Se, so only sulfhydryl sites on the cell surface are blocked, leaving sulfhydryl sites on the exudates that are produced during the experiments free to react with Se(IV). In the first of these Type 4 experiments, after the 2 h exposure of the cells to qBBr in the excess qBBr experiments, selenite was added and samples were taken as described above. In the second of these Type 4 whole-cell experiments, the same protocol was used through the qBBr treatment step, but then excess qBBr was removed from the system using the same wash protocol that was followed for the removal of the growth medium (see above). After washing, the cells were resuspended at 20 g/L and selenite was added. Comparing the results of the two types of whole-cell experiments enables us to determine if the production of exudate molecules from the cells during the experiment contributes to the overall extent of Se(IV) reduction.

Due to the observation of Se(IV) reduction by S. oneidensis in the washed Type 4 experiments and the lack of reduction in the Type 1 and unwashed Type 4 experiments involving S. oneidensis, we conducted the Type 5 series of experiments with S. oneidensis exudates. We tested whether exposure of the biomass to selenite during growth affects the reduction capability of the exudates that were subsequently produced by the cells. These experiments were conducted following the same protocol as the Type 1 experiments, except 10 mL/L of a 1000 ppm Na₂SeO₃ stock solution was added to the growth medium and to the 0.01 M NaCl solution after resuspension to achieve a concentration of 10 ppm Se(IV) during the production of the exudate solutions. Exudates were harvested using the same protocols as the Type 1 experiments, and the exudate solutions were then spiked with an additional 10 ppm of selenite. Samples were taken before the Se(IV) spike in addition to taking samples as a function of time after the spike.

2.3. Dissolved Se analyses

The reduction of selenite leads to the precipitation of solid-phase elemental Se(0) (Ganther, 1971), and hence causes removal of aqueous Se from solution. We measured the concentration of total dissolved Se in our samples, and assumed that the extent of selenite reduction that occurs in each system is quantified by the decrease in the concentration of dissolved Se. The concentration of total dissolved Se was measured in each sample using inductively coupled plasma optical emission spectroscopy (ICP-OES; Perkin Elmer Optima 8000), analyzing at a wavelength of 129.026 nm. Matrix-matched standards were prepared over a range of 0 to 20 ppm Se. Replicate analyses of standard solutions indicated that analytical uncertainty in the measured Se concentrations was \pm 5 % (1 standard deviation).

2.4. X-ray absorption spectroscopy

We used X-ray absorption spectroscopy (XAS) to determine the valence state and binding environment of the Se under conditions similar to those used in the Type 1 selenite + exudate reduction experiments. Two types of samples for XAS analysis were prepared: 1) a time series samples taken from a system with a similar Se:exudate ratio as the Type 1 experiments to probe reduction kinetics; and 2) a sample from a system with lower Se:exudate ratio to increase the proportion of potential Se-sulfhydryl species. Because sulfhydryl sites likely represent only a small fraction of the total number of binding sites on the exudate molecules, any Se-sulfhydryl binding could be overwhelmed in the XAS signal by the non-sulfhydryl Se binding. Assuming that Se has a higher affinity to bind with sulfhydryl sites than it has with the other possible binding sites, the lower Se:exudate ratio sample optimized to increase the proportion of Se-sulfhydryl binding. The first set of samples for XAS analysis were prepared using a system with the exudates produced from a suspension of 40 g/L of B. subtilis biomass, exposed to 50 ppm Se(IV). In these higher Se:exudate ratio experiments, samples were taken at 1, 24, 32, 40, and 48 h to probe the progression of the reaction over time. Another sample was prepared using a system with the exudates produced from a suspension of 40 g/L of B. subtilis biomass, exposed to only 1 ppm Se(IV), with the sample collected after 48 h of exposure. The exudates were otherwise collected and reacted as described above. Samples were frozen immediately to stop reactions and to save for lyophilization, which was done for all sets after the last sample of each set had been frozen for 24 h. After lyophilization, the headspace of the sample container was purged for 1 h with nitrogen gas to remove any oxygen and to reduce the possibility of Se re-oxidation in the sample prior to XAS analysis.

Se K-edge (12,658 eV) X-ray absorption spectroscopy measurements were conducted at the MR-CAT/EnviroCAT bending magnet beamline (Sector 10, Advanced Photon Source) (Segre et al., 2000). X-ray absorption near edge spectra (XANES) and extended X-ray absorption fine structure (EXAFS) spectra were collected in transmission and fluorescence mode using gas-filled ionization chambers. The freeze-dried solids from the Se(IV) reacted with exudates were sealed in a 1.5 mm thick plastic slide between two layers of Kapton film. All sample handling procedures were done under ambient atmosphere. Energy calibration was established by setting the inflection point in the spectrum from Se metal to 12,658 eV and was maintained afterwards by collecting data from the foil simultaneously with the collection of data from the samples. We monitored for radiation-induced changes in the spectra on the timescale of quick XANES scans lasting 20 s each. None were observed for the dried samples or the standards. No differences were observed between spectra from 3 to 5 distinct locations on the sample so all scans from each sample were averaged to produce the final spectrum.

Analyses of the spectra involved comparisons to Se standards. The standards dataset measured at the same beamline in this and previous work (Yu et al., 2018) include Na-selenate, Na-selenite, orthorhombic Se(0), selenium disulfide (SeS₂), selenocystine (COOH-CNH₂-CSe-seC-CNH₂- COOH), selenourea (Se-C-(NH₂)₂), and Se adsorbed to a thiol resin (Goff et al., 2021). The polycrystalline Se powders were mounted on the adhesive side of Kapton tape and their absorption spectra were measured in transmission mode. The thiol-adsorbed standard was packed in a 1.5 mm thick plastic slide between two layers of Kapton film. Normalization and background removal of the data was done using the program AUTOBK (Newville et al., 1993). Linear combination fits of the XANES data were performed using the program ATHENA (Ravel and Newville, 2005). Shell-by-shell fitting of the EXAFS data was

done using the program FEFFIT (Newville et al., 1995; Yu et al., 2018).

2.5. Bottom-up proteomics for protein identification

To identify the protein components of the bacterial exudate solutions, bottom-up proteomics experiments were conducted with a Thermo-Finnegan Q-Exactive HF (QEHF) mass spectrometer coupled to a Waters MClass ultrahigh pressure liquid chromatography system via a nanoelectrospray ionization source. Exudates were produced as described above, then concentrated using a 3kD molecular weight cutoff filter (Millipore-Sigma) and subjected to trypsin digestion. Between 1 and 5 µL of a sample containing tryptic peptides was eluted from an Acquity BEH C18 Column, 1.7-μm particle size, 300 Å (Waters) column (100 μm inner diameter × 100 mm long) using a 100-min gradient at a flow rate of 0.9 $\mu L/min$ (4–33 % B for 90 min, 33–80 % B for 2 min, constant at 80 % B for 6 min, and then 80-0 % B for 2 min to equilibrate the column). Data were collected in positive ionization mode. Mass spectra were acquired in the Orbitrap at 60 k resolving power and tandem mass spectra were then generated for the top seventeen most abundant ions with charge states ranging between 2 and 5. Fragmentation of selected peptide ions was achieved via high energy collisional dissociation (HCD) at normalized collision energy of 35 eV in the HCD cell of the OEHF. Proteome Discoverer 2.2 software employing either Mascot or Sequest search engines with a decoy search at a 1 % false discovery rate was used to identify proteins present in each sample by matching tandem mass spectra with peptides expected for proteins in the SwissProt database.

3. Results

The Type 1 experimental systems that contained either untreated *B. subtilis* or *P. putida* exudates exhibited an increasing extent of Se removal from solution as a function of time (Fig. 1). The most likely removal mechanism in these systems is the reduction of selenite to elemental Se(0), which causes the precipitation of characteristically red nanoparticles of Se(0) (Garbisu et al., 1996). The experimental systems containing exudates produced by *B. subtilis* or by *P. putida* both yielded suspensions with a red coloration (Fig. 2), an observation consistent with the exudates promoting Se(IV) reduction to Se(0) (Lampis et al., 2014; Wang et al., 2018). There is a 24–48 h lag observed between the start of the experiment and when significant removal of Se from solution occurs, after which the concentration of selenium in solution

decreases continuously through the 96 h timepoint (Fig. 1, panels a and b). For both of these systems, exposure of the exudates to the sulfhydryl-blocking molecule qBBr prior to the addition of selenite (Type 2 experiments) effectively eliminates Se removal from solution (Fig. 1).

In contrast, the Type 1 experimental systems containing exudates that were produced by *S. oneidensis* did not exhibit measurable Se removal from solution over 96 h, regardless of the biomass concentration that was used to produce the exudates (Fig. 1c) or whether the exudates were treated with qBBr (data not shown). The measured concentration of Se in solution remained constant over the duration of the *S. oneidensis* experiments, and no red color appeared in these solutions (Fig. 2).

The Type 3 and 4 experiments that involved whole cell biomass exhibited significantly different Se removal behavior than was measured for the exudate-only systems (Fig. 3). Solutions containing untreated bacterial biomass (filled circles in Fig. 3) exhibited relatively rapid decreases in selenium concentration over the first 8–12 h, with no apparent lag phase prior to the initiation of Se removal. The observed extents of Se removal from solution in each of the three biomass systems at 96 h were significantly greater than those measured in the systems containing only the exudates produced by the same concentration of those bacterial species. In addition, for each of the three biomass systems,

treatment of the biomass with an excess of qBBr (filled triangles in Fig. 3) led to a dramatic decrease in the rate of Se removal from solution for at least 72 h (Fig. 3). At 72 h, the qBBr-treated systems exhibited aqueous Se concentrations of at least 74 % of the initial selenium in solution. In comparison, in the untreated biomass experiments the dissolved selenium concentrations had dropped below the detection limit for this analysis by 48 h. Although the qBBr-treated *B. subtilis* system exhibited a decreased rate of Se removal until 72 h, between 72 and 96 h, the rate of Se removal increased markedly and only 31 % of the original Se remained in solution at 96 h. In contrast, the *P. putida* and the *S. oneidensis* systems exhibited roughly the same rate of Se removal between 72 and 96 h as was observed prior to 72 h.

In contrast to the systems in which excess qBBr was left in solution, for each of the three bacterial species studied, the Type 4 biomass experiments in which the excess qBBr was removed by an extra wash step prior to the addition of Se exhibited significant removal of Se (open squares in Fig. 3), to the extent that at 72 h the selenium concentrations measured were a maximum of 12 % of the initial concentrations, and at 96 h all of these qBBr-treated systems had selenite concentrations below the limit of detection.

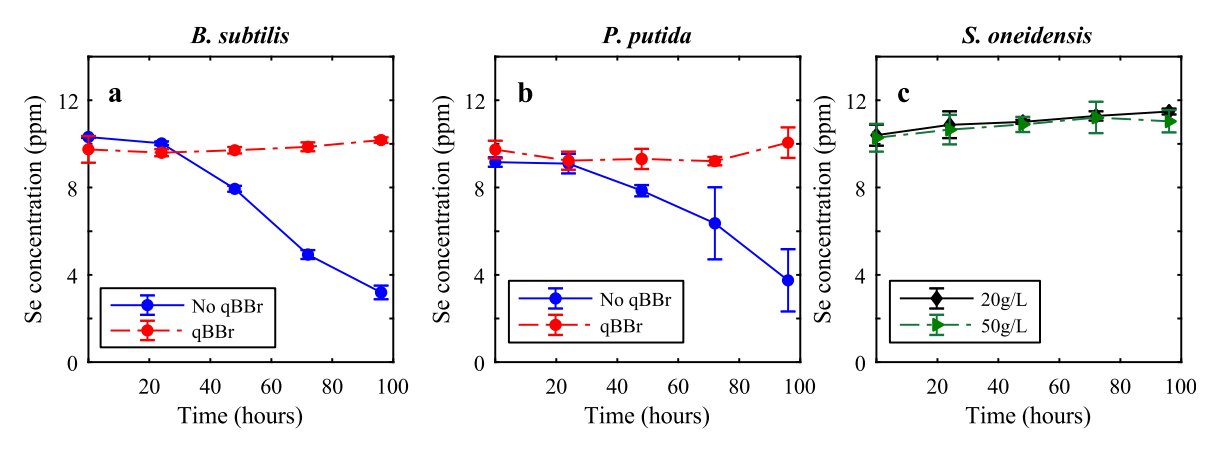


Fig. 1. Removal of dissolved selenium as a function of exposure time in the presence of exudates produced by 20 g/L of a) *B. subtilis* biomass and b) *P. putida* biomass, both with (dashed line) and without (solid line) qBBr treatment; and c) exudates produced by *S. oneidensis* at a concentration of 20 and 50 g of biomass/L. Error bars show one standard deviation



Fig. 2. Experimental systems involving exudate produced by a) *B. subtilis*, b) *P. putida*, and c) *S. oneidensis* (vial pairs, left to right) at a concentration of 20 g biomass/L and an initial [Se] of 10 ppm at 0 h (left vial in pair) and 96 h (right vial in pair), demonstrating the appearance over time of a red coloration to the solution as selenite is reduced to elemental Se(0) by *B. subtilis* and *P. putida* exudates. N.B. the exudates produced by *S. oneidensis* biomass have an orange tint when harvested as the biomass is red–orange as compared to *B. subtilis* and *P. putida* biomass, which are beige-white. The coloration is not a result of Se(IV) addition.

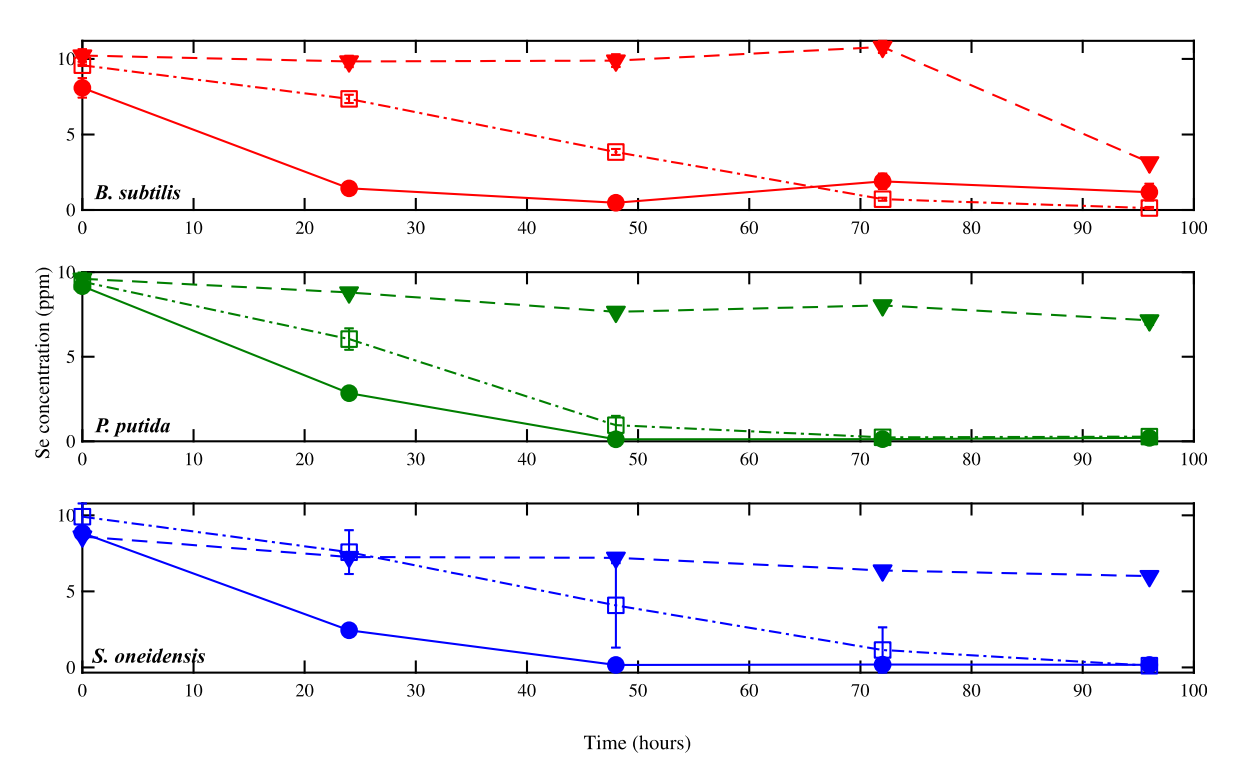


Fig. 3. The concentration of Se remaining in solution as a function of time when exposed to bacterial biomass (from top to bottom panel: a) *B. subtilis*, b) *P. putida*, c) *S. oneidensis*) at a concentration of 20 g/L. Samples not treated with qBBr are plotted with solid curves/filled circles; samples treated with qBBr and not washed are plotted with dashed lines/filled triangles; and samples treated with qBBr and washed to remove excess are plotted with dot-dashed lines/open squares. Error bars show one standard deviation.

Of particular note, these washed Type 4 experiments showed a capacity for reduction by *S. oneidensis* exudates (Fig. 4, panel c, open squares) not observed in Types 1 or 2 experiments involving *S. oneidensis*. In contrast to the *S. oneidensis* exudates which were produced from cells grown in a Se-free medium and which showed no evidence of Se(IV) reduction at concentrations of either 20 or 50 g/biomass per liter (Fig. 1), exudates produced from a 20 g/L cell suspension using cells grown in a medium containing 10 ppm Se

(IV) demonstrated significant removal of Se from solution over the course of 96 h (Fig. 4).

To determine the relative importance of exudates and whole cells in Se(IV) reduction, we calculated mass-normalized first-order rate constants for each dataset, using the measurements of Se concentration taken during the period of most rapid Se removal from solution for each experiment. For each set of experiments, the In[Se] was plotted as a function of time, and a linear fit was

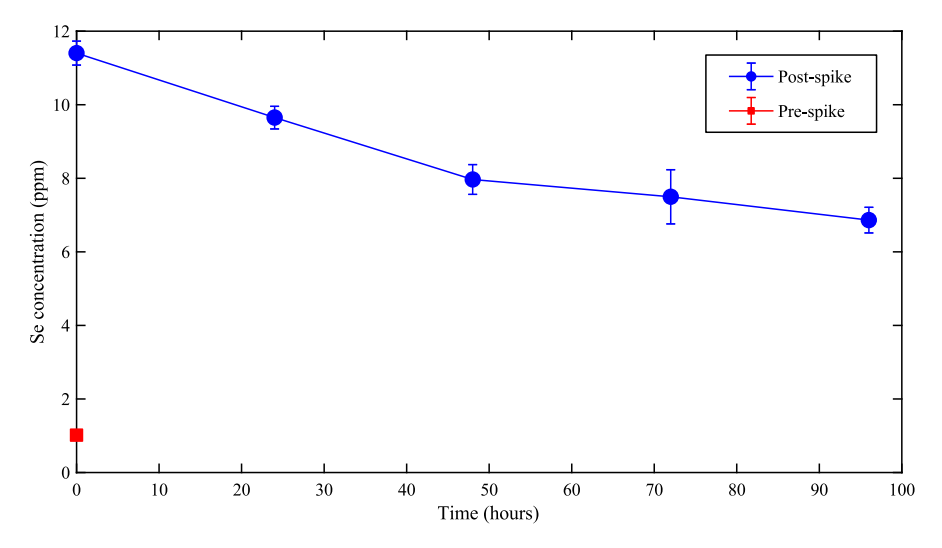


Fig. 4. Concentration of selenium remaining in solution over time when exposed to exudates produced by 20 g/L S. oneidensis biomass that was grown in the presence of 10 ppm Se(IV) (Type 5 experiments). The red square is the measured concentration of Se remaining in solution after the growth phase and prior to the experiments. The blue circles are the measured concentrations of Se remaining in solution after a 10 ppm Se(IV) spike to start the experimental phase at time = 0.

applied; in each case, the data are well-approximated by the linear fits (Figure S2). For each experiment, a value for the reduction rate constant, k, was calculated as the negative slope of the linear fit to the data points, and we normalized these values either to the biomass used in the experiment (for the whole-cell biomass experiments) or to the mass of the bacteria used to generate the exudate solution (for the exudate-only experiments).

The calculated rate constant values (Table 1) indicate that, for each of the bacterial species studied, the whole cell biomass removed selenium from solution more quickly than did the exudates produced from a corresponding mass of cells. It is important to note that the calculated rate constants are the minimum values for the rate of reduction; more frequent sampling intervals over the first 24 h could define a faster reduction rate, especially for the whole cell biomass experiments. Additionally, we are only able to measure Se removal as a proxy for Se(IV) reduction. As discussed above, it is possible that reduction of Se(IV) outpaces Se removal from solution due to the inability of our approach to separate monodisperse Se(0) nanoparticles from the experimental solution.

The reduction of Se(IV) was measurable by X-ray absorption near edge structure (XANES) and extended X-ray absorption fine structure (EXAFS) analyses in the 40 and 48 h *B. subtilis* high Se:exudate ratio samples, and was more pronounced in the low Se:exudate ratio sample where a larger proportion of the Se atoms were transformed. Fig. 5 compares the XANES spectra from the Seexudate samples to that from various Se standards.

Table 1Calculated rate constants for exudate-only and whole-cell experiments.

Mass normalized k value ^a	
B. subtilis	
Exudate only	2.2×10^{-7}
Whole cell	8.2×10^{-7}
P. putida	
Exudate only	1.7×10^{-7}
Whole cell	2.1×10^{-6}
S. oneidensis	
Exudate only	No removal
Whole cell	1.3×10^{-6}

^a Units for normalized rate constant k are L s⁻¹ g⁻¹. For the exudate-only experiments for each species, we used 24, 48, 72, and 96 h measurements to define the k value; for the whole-cell biomass experiments we used the 0, 24, and 48 h measurements, due to the relatively rapid rate of Se removal in these systems.

The energy position of the absorption edge is indicative of the average valence of Se, with lower positions corresponding to reduced valence and higher positions indicating oxidized valence states (Ryser et al., 2005; Olegario et al., 2010). The spectra of the high Se: exudate ratio samples from 1 h to 32 h are nearly identical to the sodium selenite standard (Na₂SeO₃, feature "b"), which indicates that Se remains predominantly as O-coordinated Se(IV) in the SeO₃ anion. The spectral trends in the 48 h sample and in the low Se:exudate sample are in the direction of the reduced Se (0) or organoselenium standards (i.e., the development of a shoulder at "c" and the suppression of peak "b"). Fig. 5 illustrates that the latter standards have similar spectral shapes and edge positions. This has also been observed in prior work where a larger number of inorganic and organic selenium standards were examined (Ryser et al., 2005; Olegario et al., 2010), revealing that several organoselenium complexes of various valences, as well as several inorganic Se(-II) standards have similar edge positions as Se(0). The spectral similarity may be due to the similarity in the nearneighbor coordination around Se in the Se(0), thiol-associated Se, the organoselenium compounds, and the SeS₂ standards, which have two Se, two S, or a combination of Se, C, and/or S atoms as near-neighbors, respectively (Wyckoff, 1963; Steudel Laitinen, 1982; Görbitz et al., 2015; Luo and Dauter, 2017). Regardless of whether this effect in the Se XANES data is due to structural or electronic factors, it limits our ability to distinguish reliably between metallic Se and Se coordinated to thiol or other organic groups. We have consequently relied on EXAFS to resolve the speciation of the final Se species (next section) and used the XANES data only to quantify the extent of transformation of the original Se(IV) species.

Linear combination fits of the XANES data indicate that for reaction times less than 40 h, the extent of Se(IV) reduction is undetectable (i.e., less than5–7 %). In the 48 h high Se:exudate ratio sample and in the low Se:exudate sample about 23 % and 63 %, respectively, of the Se(IV) species were transformed to lower-valence or organo-coordinated Se (Fig. 5, Table S1). The XANES measurement of 23 % transformation in the 48 h sample is consistent with our observation of \sim 8 ppm Se remaining in solution at 48 h in the system containing *B. subtilis* exudates (Fig. 1a). No evidence for oxidation to Se(VI) by the cell exudates was found in the XANES data (i.e., no peak appearing along line "a", Fig. 5), in contrast to the oxidation of Se(IV) to Se(VI) observed by Yu et al.

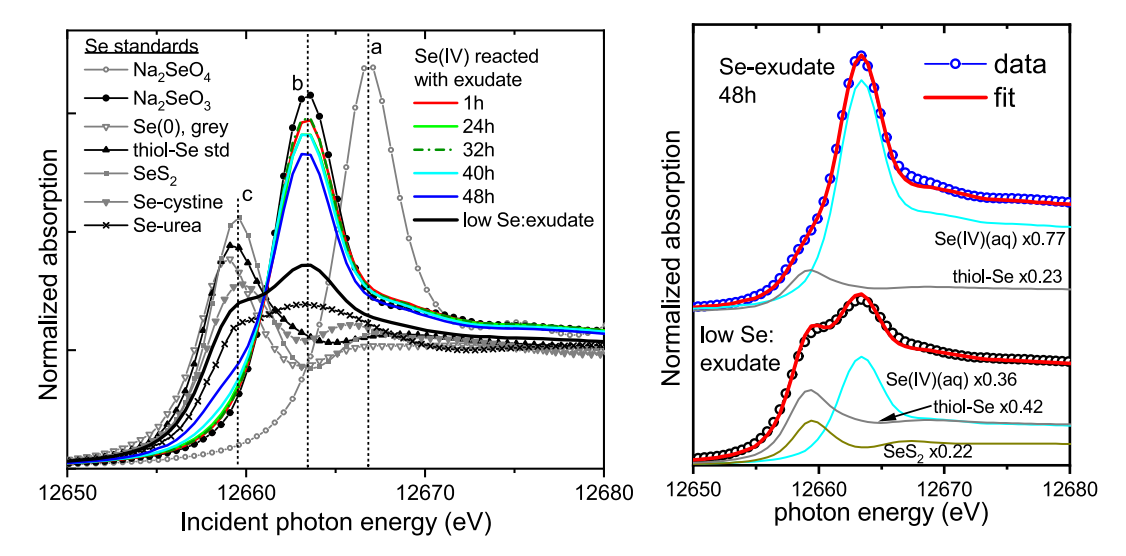


Fig. 5. Left: Comparisons between the Se K-edge XANES spectra from the standards and the Se:exudate samples. Right: LC fits of the 48 and the low Se:exudate sample, quantifying the transformations of the initial Se(IV) species. The scaled spectral components in the fit are also shown together with the weight factor. The dashed lines labeled 'a', 'b', and 'c' denote peak locations for the Na₂SeO₄, the Na₂SeO₃, and reduced S standards, respectively.

(2018) with *B. subtilis* biomass. This is consistent with the mechanism proposed for the oxidation reaction within that work, which required the presence of both nitric oxide and superoxide species generated by the bacterial biomass. Without bacterial biomass present in our exudate systems, oxidation of Se(IV) to Se(VI) does not occur

The trends in the EXAFS data are consistent with the findings from the XANES analyses (Fig. 6, see the qualitative discussion in the SI). A quantitative shell-by-shell analysis of the EXAFS data for the standards and for the Se:exudate samples enables us to place more rigorous constraints on the Se speciation in the samples. Fits of the aqueous Se(IV), thiol-adsorbed Se, metallic Se(0), and the organo-selenium standards establishes the spectral features and parameters characteristic of O, S, Se, C, and N coordination around Se, respectively (see the SI for a detailed description of the fitting procedures and results for the Se standards). The calibrated contributions of these paths in the EXAFS of the standards were used to quantify the relative content of Se-O, Se-S, Se-Se, Se-C, and Se-N coordination in the spectra of the Se:exudate ratio samples, which were then interpreted as the proportions of selen-

ite $(Se(IV)O_3)$ remaining in the lyophilized exudate solids, thiolassociated Se species, reduced Se(0) species, and organoselenium species, respectively.

Fig. 6 shows that the 1 to 40 h high Se:exudate ratio samples yield EXAFS spectra that are nearly identical to that of the aqueous selenite standard and are correspondingly modelled well with a single O shell (Figure S1 and Table S2, fits B-F). This indicates that the starting Se(IV) species remained predominantly untransformed for 40 h. The 48 h sample shows additional amplitude around R + Δ = 2.0 Å remaining after the fit with an O shell (Figure S1, fit G). The additional peaks can be modeled with either a S or a Se shell, producing similar improvements in the fit relative to the O shell fit alone (Table S2, fits H and I). However, the slightly better fit with a Se shell at 2.39 Å suggests the precipitation of metallic Se, consistent with the change in color of the suspension (Fig. 2). The proportion of SeO₃ species that transformed to S-coordinated species (25 %= 0.4/1.6, ± 10 %, obtained by scaling the refined coordination number to that in the standard) in the 48 h sample is consistent with the 25 % loss in starting Se species determined by linear combination fits of the XANES data (Table S1). Fits with both S and Se

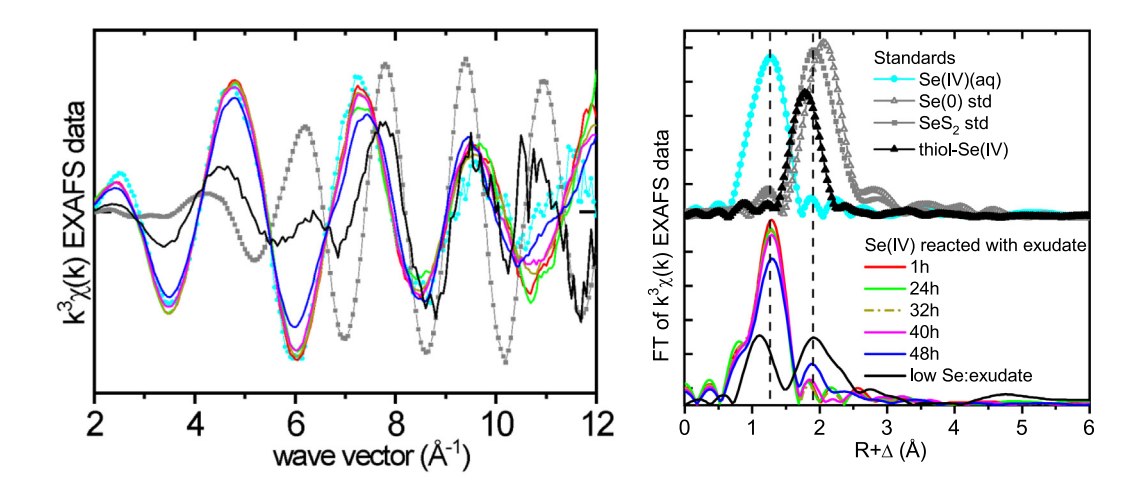


Fig. 6. Left: Left: Se K-edge EXAFS spectra from the high Se:exudate ratio samples reacted for 1–48 h and from the low Se:exudate ratio sample (lines), compared to standards (symbols). Right: Magnitude of the Fourier transform of the data in the left figure. The line convention is the same in both figures, not all standards are included in the left figure for clarity. The vertical dashed lines delineate the position of peaks attributable to O (left) or S/Se (right) coordination in the standards.

shells were not successful due to the overlap between the two signals resulting in parameter correlations and refined coordination numbers that were consistent with 0 (e.g., 0.2 ± 0.5), so the presence of both S- and Se-coordinated species at 48 h could not be resolved. In contrast, the outer-shell features in the sample with low Se:exudate ratio were of significantly higher amplitude (Fig. 6), consistent with the increased proportion of transformed Se species determined by the analysis of the XANES data (Table S1). An EXAFS model with Se-O, Se-S, and Se-Se paths provides the best reproduction of the data (Figure S1 and Table S2, fit I). The refined coordination numbers can be scaled to those in the standards and interpreted as that sample having approximately 36 % (=0.86/2.4, ± 10 %) of the Se atoms remaining as adsorbed SeO₃, 29 % (=0.46/1.6, ± 10 %) of the Se atoms coordinated to S atoms as in the thiol standard, and about 41 % (=0.52/1.3, ±10 %) coordinated to other Se atoms as in the cystine standard. Unfortunately, the overlap of signals from three different Se species in the spectrum of the low Se:exudate sample does not allow for isolation and a more detailed analysis of the S-coordination environment, so questions such as whether the transformed Se was sequestered as monosulfide or disulfide Se species cannot be addressed (Steudel and Laitinen, 1982).

Our experimental data indicate that sulfhydryl sites on bacterial exudate molecules are directly involved in the process of Se(IV) reduction, and that blockage of the sulfhydryl sites by qBBr effectively stops Se(IV) reduction by the exudates. Therefore, we conducted a proteomics analysis of exudate solutions from each bacterial species in order to constrain the potential host molecules of the sulfhydryl sites and to identify initial candidate proteins responsible for the observed Se(IV) reduction. Table 2 lists a subset of identified proteins with at least one redox active sulfhydryl site in the exudate solution from each bacterial species according to SwissProt annotations. This screening was solely for identification purposes, not quantitation, and as such we cannot compare relative abundances of proteins. An additional file containing a complete list of proteins identified in each species is provided in Supplemental Materials.

4. Discussion

The results from the exudate-only experiments demonstrate for the first time that bacterial exudates from the species *B. subtilis* and

Table 2 Identified peptides with at least 1 redox-active sulfhydryl site.

Accession No.	Protein	Gene
B. subtilis		
P21880	Dihydrolipoyl dehydrogenase (EC 1.8.1.4)	pdhD
P80864	Thiol peroxidase (Tpx) (EC 1.11.1.24)	tpx
P14949	Thioredoxin (Trx)	trxA
P54533	Dihydrolipoyl dehydrogenase (EC 1.8.1.4)	bfmBC
P80880	Thioredoxin reductase (TRXR) (EC 1.8.1.9)	trxB
P. putida		
Q839B0	33 kDa chaperonin (Heat shock protein 33 homolog) (HSP33)	hslO
032823	Thioredoxin reductase (TRXR) (EC 1.8.1.9)	trxB
S. oneidensis		
P43784	Dihydrolipoyl dehydrogenase (EC 1.8.1.4)	lpdA
Q9KSS4	Thioredoxin reductase (TRXR) (EC 1.8.1.9)	trxB
Q9KPF6	Dihydrolipoyl dehydrogenase (EC 1.8.1.4)	lpd
Q8EKD2	33 kDa chaperonin (Heat shock protein 33 homolog) (HSP33)	hslO
Q89AS4	Ribonucleoside-diphosphate reductase subunit alpha (EC 1.17.4.1)	nrdA
P43754	Ribonucleoside-diphosphate reductase subunit alpha (EC 1.17.4.1)	nrdA
P0AA27	Thioredoxin 1 (Trx-1)	trxA

P. putida can promote the reduction of Se(IV) to elemental selenium. In addition, it is evident that the range of this capacity varies widely between bacterial species. Bacterial exudates have been shown to also promote the reduction of aqueous Au(III) (Kenney et al., 2012), so these findings suggest that this source of electrons could play a significant role in the environmental fate of other redox-active elements as well. Exudate reduction of Se(IV) requires both the binding of Se(IV) onto the exudate molecules and electron transfer from the exudate molecules to the bound Se(IV) atoms. Like bacterial surfaces, bacterial exudates contain plentiful organic acid functional groups, which under the experimental pH conditions are predominantly deprotonated and negatively charged (Seders and Fein, 2011). Electrostatic repulsion between the negatively-charged aqueous selenite and negatively-charged carboxyl and other oxygen-based ligands on the exudate molecules makes it unlikely that these types of functional groups are involved in selenite binding onto the exudate molecules. In fact, our data indicate that the binding is accomplished via Se-sulfhydryl binding, similar to the mechanism of selenite adsorption onto bacterial cell surfaces (Yu et al., 2018). That is, the addition of qBBr, which effectively and irreversibly blocks sulfhydryl sites to further binding by Se, to the experimental systems that contain B. subtilis or P. putida exudates leads to a cessation of Se(IV) reduction.

Our XAS data, together with the qBBr site blocking experiments, support the conclusion that Se(IV) must bind to a sulfhydryl site on the exudate molecules for electron transfer to occur. The XANES and the EXAFS results for the 48 h B. subtilis high Se:exudate ratio sample and for the low Se:exudate ratio sample show evidence for the presence of both thiol-associated selenium atoms and elemental nanoparticulate selenium, which confirm Se(IV) reduction and indicate Se association with sulfhydryl sites. Se(0) nanoparticles are also visually evident in the B. subtilis and P. putida exudateonly experiments, as they cause the solution to turn a characteristic cloudy red color (Fig. 2). The fact that Se-S coordination is most clearly detected by XAS under low Se loading conditions suggests that sulfhydryl sites make up only a small minority of the total concentration of binding sites on the exudate molecules. Under our higher Se loading conditions, the concentration of sulfhydryl sites is too small relative to the concentration of Se in the sample to reduce enough of the total selenium present for Se-S binding to be detectable via XAS over the examined timeframe. However, it is possible that reduction of the excess Se could occur at sulfhydryl sites in a cyclic fashion over extended time. Although these sulfhydryl sites appear to comprise a minor fraction of the proton-active sites on the exudates, the dramatic effect of the qBBr treatment on Se(IV) reduction demonstrates that these sites play a critical role in the reduction process.

The importance of exudate sulfhydryl sites in the Se(IV) reduction process helps to explain the absence of reduction that we observed in the experiments involving S. oneidensis-derived exudates (Fig. 1c). When grown in the absence of Se(IV), both B. subtilis and P. putida biomass contain significant concentrations of sulfhydryl sites on their exuded EPS molecules, while S. oneidensis does not (Yu and Fein, 2016). Rather, all detectable sulfhydryl sites on S. oneidensis are located on the cell surface. Therefore, very few or no sulfhydryl sites are present on the S. oneidensis exudate molecules, and hence even if S. oneidensis exudate molecules could serve as electron donors to Se(IV), the lack of sulfhydryl binding sites on the molecules prevents Se(IV) atoms from attaching to the molecules and no selenite reduction is possible. The stark contrast in reduction behaviors displayed by exudates of B. subtilis and P. putida relative to that exhibited by S. oneidensis exudates underscores the importance of sulfhydryl site availability to the reduction process (Kenney and Fein, 2011b).

Our data also indicate for the first time that growth conditions can affect the ability of bacterial exudates to reduce Se(IV), likely

by increasing the sulfhydryl site concentration of exudates produced by cells grown in the presence of Se(IV). We observed that S. oneidensis exudates can reduce selenite only when the exudates are produced by cells grown in the presence of 10 ppm Se(IV). This result indicates that at least some bacterial species control the composition of their exudate molecules, and hence their capacity for Se(IV) reduction, through a regulatory control. Further studies are required to understand the full scope and mechanisms of this control, but it is clear that in some cases this behavior can be induced by environmental conditions. Our results do not constrain whether the distribution of sulfhydryl sites between the biomass and the exudates changes as a function of cell growth condition but given the crucial role of sulfhydryl sites to Se(IV) reduction that we observed in our experimental systems, such dependence is likely. Previous experiments demonstrate that growth conditions exert a direct impact on sulfhydryl site concentrations on biomass (Yu and Fein, 2017: Butzen and Fein, 2021).

Our whole-cell biomass experimental results differ from those in the exudate-only systems in both the timing and extent of the observed Se(IV) reduction. In contrast to the ~ 24 –48 h lag in the onset of Se removal that we observed in the exudate-only systems, removal of Se in the three whole-cell systems is more rapid, with significant Se removal observed at 24 h in the presence of bacterial biomass. The more rapid removal of Se from solution in the biomass systems relative to what we observed in the exudate-only systems may be caused by a number of factors. Bacterial cells may contain a higher concentration of sulfhydryl sites and capacity for electron transfer to Se(IV) than the exudate molecules. Conversely, the presence of the cells and subsequent centrifugation of the cells during sampling could be facilitating Se removal in the biomass systems either by Se(IV) adsorption onto the cell surfaces or by adhesion of any Se(0) nanoparticles that form as a result of Se(IV) reduction to the bacterial biomass, all of which is then centrifuged out of suspension. In the exudate-only experiments, the initial Se(0) nanoparticles to form are either monodisperse or attached to soluble exudate molecules, neither of which are removed by our centrifugation procedure, and measurable Se removal from solution only can occur after Ostwald ripening of the Se(0) nanoparticles. The development of Se nanoparticles through an Ostwald ripening process can cause a delay of greater than 24 h between the depletion of Se(IV)O₃ from solution and the formation of detectable Se(0) nanoparticles (Lampis et al., 2014). Hence, the observed extents and rates of Se(IV) reduction that we report from the exudate-only experiments are likely minimum values only, and the actual extent and rate of Se(IV) reduction in these systems could be higher than our experiments indicate. However, the fact that we do not detect Se(0) in the 24 or 32 h XAS samples at a similar Se:exudate ratio indicates that if Se(IV) reduction occurred in these systems, its maximum extent would be approximately 5–7 % of the total Se present as this is the detection limit for the XAS approach.

We hypothesize that the bacteria in the whole cell biomass experiments produce exudate molecules during the course of the experiments, and that these exudates can promote further Se(IV) reduction if any Se(IV) is left in solution. In the *P. putida* and *S. oneidensis* biomass experiments, there is little Se(IV) remaining in solution after the first stage of Se(IV) reduction for these exudates to reduce. However, in the *B. subtilis* biomass experiments, removal appears to plateau for a period before resuming. We attribute this plateau to limited surface-site availability; sufficient exudates must be produced to allow reduction to continue by providing more reactive sites.

When excess qBBr was left in the system (filled triangles in Fig. 3), the sulfhydryl sites on the bacterial surfaces and on the exudate molecules which were produced during the experiment could both be blocked, and hence the rate of Se(IV) reduction was greatly

decreased. This decreased rate of removal of Se in the excess qBBr experiments continued for at least 96 h in the *P. putida* and the *S.* oneidensis systems, however the B. subtilis experiments that had excess gBBr exhibited an increased rate of Se removal between 72 and 96 h. It is likely that after 72 h in these experiments, the concentration of released exudates from the bacterial cells reached a level that exceeded that of qBBr remaining in solution, enabling the exudates to reduce Se(IV). Conversely, when the excess qBBr was removed from the system prior to the addition of Se, the bacterial surface sulfhydryl sites were blocked, but the sulfhydryl sites on the exudates that were produced during the experiment were not. In these experiments, the qBBr treated systems exhibited lower initial Se(IV) removal. However, by 96 h the selenium levels in solution in the systems had decreased below the limit of detection, regardless of whether the system had been initially treated with gBBr (open squares, Fig. 3), likely due to production of new exudates capable of Se(IV) reduction during the rest of the experiment. As discussed above, the introduction of Se(IV) in the growth and soaking phases of exudate preparation from S. oneidensis biomass likely altered the composition of the exudates produced such that selenite reduction could occur. These conditions are similar to the conditions of the qBBr-treated, Type 4 experiments which contained cells with excess qBBr removed by washing, and the results provide an explanation for the reduction observed in those experiments (open symbols in the bottom panel of Fig. 3). That is, S. oneidensis cells when exposed to Se(IV) during the Type 4 experiments must have produced exudates similar to those produced during the Type 5 experiments which involved the presence of Se(IV) in the growth medium, and the exudates produced in both of these systems were capable of Se(IV) reduction. Our experimental results indicate that exudates from S. oneidensis cells can only reduce significant concentrations of Se(IV) when Se(IV) is present with the cells as the exudates are produced, again supporting a regulatory process that controls exudate sulfhydryl site concentrations, at least for S. oneidensis.

For B. subtilis, the whole cell biomass system removed Se(IV) from solution nearly 3 times faster than the exudate-only system: for P. putida, the ratio was 4 times faster; and for S. oneidensis, the whole cell biomass exhibited the fastest Se(IV) removal rate observed in this study, while the exudate-only system had no measurable Se(IV) removal, unless the biomass was grown and soaked in the presence of Se(IV). Therefore, our results suggest that although there is a range of behaviors, Se(IV) reduction is predominantly controlled by the bacterial biomass, rather than by exudates when electron availability is not limited. The role of both bacterial cells and exudates in Se(IV) reduction likely depends on electron donor availability. In our experimental systems, the bacterial cells and the exudates produced from the cells have plentiful electrons due to loading of the electron transport chain during cell metabolism in the rich medium in which they are grown. Natural soil and groundwater systems contain both whole-cell biomass as well as exuded substances. While our data suggest that bacterial biomass is generally capable of promoting faster reduction rates than exudates alone on a mass normalized basis in nutrient rich systems where electron donors are present in great excess, it is possible that exudate-mediated reduction could be dominant in conditions where electron donors are more limited. For example, the cells in the B. subtilis whole cell biomass experiment appear to have a limited capacity for Se(IV) reduction, and after approximately 72 h, Se(IV) reduction becomes dominantly exudatepromoted.

The calculated rate constants demonstrate that the importance of bacterial exudates to Se(IV) reduction varies markedly between species, and that while sulfhydryl site concentrations account for some of these differences, other factors must also exert an influence. Exudates from *P. putida* and *B. subtilis* promote relatively

rapid Se(IV) reduction compared to the rate of reduction promoted by S. oneidensis exudates. These observed differences likely stem from differences in sulfhydryl site concentrations on the exudate molecules, as P. putida and B. subtilis exudates each have significantly higher concentrations of sulfhydryl sites than does S. oneidensis, whose sulfhydryl sites, when grown in the absence of Se (IV), are located primarily on the cell surface (Yu and Fein, 2016). Of the three species studied here, the S. oneidensis cell surface has the highest concentration of sulfhydryls on its surface, but P. putida has the lowest concentration, so the observed reduction rates do not correlate directly with cell surface sulfhydryl site concentrations. The configuration of sulfhydryl sites on the cell surface may differ between the studied bacterial species, and steric configurations between Se(IV) and the sulfhydryl sites may account for the observed differences in reduction rate. More detailed spectroscopic work is needed to test these hypotheses.

To understand the differences observed in reduction characteristics between whole-cell and exudate-only conditions, as well as between bacterial species, it is important to consider the likely mechanisms of reduction. Multiple mechanisms for bacterial reduction of selenite have been established, both intracellularly and extracellularly, including a Painter-type reaction and reactions with various terminal reductases (Hunter, 2014; Song et al., 2017; Wang et al., 2018). Specifically, thioredoxin reductase and fumarate reductase have been implicated in bacterially-mediated selenite reduction in several in vivo experiments. Additionally, purified glutathione reductase has been shown to reduce selenite in vitro in the presence of NADPH (Ganther, 1971; Ni et al., 2015). Thioredoxin reductase and glutathione reductase, both within the flavoprotein disulfide reductase family, have conserved catalytic cysteine residues within their active sites (Sustmann et al., 1989; Kouwen et al., 2008). In contrast, fumarate reductase catalytic activity is dependent on an arginine residue within the active site (Reid et al., 2000). It is, therefore, possible that the shutoff of Se(IV) reduction achieved by gBBr treatment in our experimental systems is due to blocking of the active site in either thioredoxin reductase or glutathione reductase, which have both been previously reported to mediate selenite reduction (Hunter, 2014; Wang et al., 2018). Thioredoxin reductase was identified in our proteomics analyses of the exudates from all three species studied here (Table 2), and although we cannot yet confirm this to be the relevant mechanism, the presence of this reductase in the experimental exudate solutions makes this a plausible mechanism. Because the qBBr blocking is sulfhydryl specific, our findings suggest that under our experimental conditions selenite reduction is not fumarate-reductase dependent, as the qBBr blocking agent should have no effect on the catalytic arginine residue. Additionally, qBBr is known to react with glutathione (Kosower and Kosower, 1987), a common cellular antioxidant and substrate for the Painter-type reaction of Se. It is therefore possible that qBBr treatment could interrupt Painter-type reduction of Se as well by blocking sulfhydryl sites on glutathione or glutathione analogues such as bacillithiol.

5. Conclusions

This study provides the first evidence that some bacterial exudates can promote Se(IV) reduction, and that similar to what occurs on bacterial surfaces, the reduction reaction is mediated by Se(IV) binding onto sulfhydryl sites. In addition, we show that this capability can be induced by environmental conditions during cell growth, suggesting regulation of this capability in at least some cases. Although more work is required to understand these regulatory mechanisms, this could have promising implications for optimizing bacterial remediation of selenium contamination.

Blocking of cell surface and exudate-bearing sulfhydryl sites with qBBr effectively stops Se(IV) removal from the experimental solutions, providing strong evidence that sulfhydryl site binding is involved in Se(IV) reduction by both whole bacterial cells and by exudates alone. Our XAS data also support a mechanism involving Se(IV) binding onto sulfhydryl sites on the exudate molecules, followed by reduction and precipitation as Se(0) nanoparticles. The bacteria that we used in this study exhibit variability in the distribution of sulfhydryl sites between the cell surface and exudate molecules, with a corresponding variability in Se(IV) reduction rates and extents. It is likely that a similar range of variability in reduction rates and extents by bacterially produced exudate molecules occurs in complex natural and engineered settings. The relative importance of cell-surface Se(IV) attachment and reduction compared to that which occurs on exudate molecules likely is controlled by the distribution of sulfhydryl sites between the cell surface and exudate molecules. In our whole-cell biomass experiments, we observed that whole cell biomass exhibits a faster rate of reduction on a per-gram basis compared to exudates alone. Differences in behavior between bacterial species does not appear to be controlled simply by the concentrations of cell surface sulfhydryl sites relative to exudate molecule sulfhydryl sites. However, our results suggest that the contributions of both soluble bacterial exudates and whole cell biomass can affect Se(IV) reduction, and both should be considered when modeling Se cycling in the environment

Data availability

Data will be made available on request.

Declaration of Competing Interest

The authors declare that they have no known competing financial interests or personal relationships that could have appeared to influence the work reported in this paper.

Acknowledgements

Funding for this study was provided by U.S. National Science Foundation grants EAR-1904192 and EAR-2149717. The ICP analyses were conducted at the Center for Environmental Science and Technology (CEST) at University of Notre Dame. This research used resources of the Advanced Photon Source, a U.S. Department of Energy (DOE) Office of Science User Facility, operated for the DOE Office of Science by Argonne National Laboratory under Contract No. DE-AC02-06CH11357. We thank the MRCAT beamline staff for assistance during data collection at the synchrotron as well as William Boggess for assistance in collection and analysis of proteomics data. MIB and KMK were supported by the Argonne Wetlands Hydrobiogeochemistry Scientific Focus Area funded by the Environmental System Science Program, Office of Biological and Environmental Research, Office of Science, U.S. Department of Energy (DOE), under contract DE-AC02-06CH11357. MRCAT/ EnviroCAT operations are supported by DOE and the MRCAT/ EnviroCAT member institutions. Two constructive and thorough journal reviews of the manuscript significantly improved the presentation of the work and are appreciated.

Appendix A. Supplementary material

Supplementary material to this article can be found online at https://doi.org/10.1016/j.gca.2022.10.014.

References

- Butzen, M.L., Fein, J.B., 2021. Electron Donor Effects on Bacterial Surface Sulfhydryl Site Concentrations. Geomicrobiol. J. 38, 294–303.
- Ganther, H.E., 1971. Reduction of the selenotrisulfide derivative of glutathione to a persulfide analog by glutathione reductase. Biochemistry 10, 4089–4098.
- Garbisu, C., Ishii, T., Leighton, T., Buchanan, B.B., 1996. Bacterial reduction of selenite to elemental selenium. Chem. Geol. 132, 199–204.
- Goff, J.L., Wang, Y., Boyanov, M.I., Yu, Q., Kemner, K.M., Fein, J.B., Yee, N., 2021. Tellurite Adsorption onto Bacterial Surfaces. Environ. Sci. Technol.
- Görbitz, C.H., Levchenko, V., Semjonovs, J., Sharif, M.Y., 2015. Crystal structure of seleno-l-cystine di-hydro-chloride. Acta. Crystallogr. E Crystallogr. Commun. 71, 726–729.
- Hunter, W.J., 2014. Pseudomonas seleniipraecipitans proteins potentially involved in selenite reduction. Curr. Microbiol. 69, 69–74.
- Joe-Wong, C., Shoenfelt, E., Hauser, E.J., Crompton, N., Myneni, S.C.B., 2012. Estimation of reactive thiol concentrations in dissolved organic matter and bacterial cell membranes in aquatic systems. Environ. Sci. Technol. 46, 9854– 9861.
- Kenney, J.P.L., Fein, J.B., 2011a. Cell wall reactivity of acidophilic and alkaliphilic bacteria determined by potentiometric titrations and Cd adsorption experiments. Environ. Sci. Technol. 45, 4446–4452.
- Kenney, J.P.L., Fein, J.B., 2011b. Importance of extracellular polysaccharides on proton and Cd binding to bacterial biomass: A comparative study. Chem. Geol.
- Kenney, J.P.L., Song, Z., Bunker, B.A., Fein, J.B., 2012. An experimental study of Au removal from solution by non-metabolizing bacterial cells and their exudates. Geochim. Cosmochim. Acta 87, 51–60.
- Kosower, N.S., Kosower, E.M., 1987. Thiol labeling with bromobimanes. Methods Enzymol. 143, 76–84.
- Kouwen, T.R.H.M., Andréll, J., Schrijver, R., Dubois, J.-Y.-F., Maher, M.J., Iwata, S., Carpenter, E.P., van Dijl, J.M., 2008. Thioredoxin A active-site mutants form mixed disulfide dimers that resemble enzyme-substrate reaction intermediates. J. Mol. Biol. 379, 520–534.
- Lampis, S., Zonaro, E., Bertolini, C., Bernardi, P., Butler, C.S., Vallini, G., 2014. Delayed formation of zero-valent selenium nanoparticles by Bacillus mycoides SelTE01 as a consequence of selenite reduction under aerobic conditions. Microb. Cell Fact. 13, 35.
- Li, D.-B., Cheng, Y.-Y., Wu, C., Li, W.-W., Li, N., Yang, Z.-C., Tong, Z.-H., Yu, H.-Q., 2014. Selenite reduction by Shewanella oneidensis MR-1 is mediated by fumarate reductase in periplasm. Sci. Rep. 4, 3735.
- Luo, Z., Dauter, Z., 2017. Embarras de richesses It is not good to be too anomalous: Accurate structure of selenourea, a chiral crystal of planar molecules. PLoS ONE 12. e0171740.
- Masscheleyn, P.H., Delaune, R.D., Patrick, H.W., 1990. Transformations of Selenium As Affected by Sediment Oxidation-Reduction Potential and pH. Environ. Sci. Technol. 24, 91–96.
- Newville, M., Livins, P., Yacoby, Y., Rehr, J.J., Stern, E.A., 1993. Near-edge x-rayabsorption fine structure of Pb: A comparison of theory and experiment. Phys. Rev. B: Condens. Matter 47, 14126–14131.
- Newville, M., Ravel, B., Haskel, D., Rehr, J.J., Stern, E.A., Yacoby, Y., 1995. Analysis of multiple-scattering XAFS data using theoretical standards. Physica B Condens. Matter 208–209, 154–156.
- Ni, T.W., Staicu, L.C., Nemeth, R.S., Schwartz, C.L., Crawford, D., Seligman, J.D., Hunter, W.J., Pilon-Smits, E.A.H., Ackerson, C.J., 2015. Progress toward clonable inorganic nanoparticles. Nanoscale 7, 17320–17327.

- Olegario, J.T., Yee, N., Miller, M., Sczepaniak, J., Manning, B., 2010. Reduction of Se (VI) to Se(-II) by zerovalent iron nanoparticle suspensions. J. Nanopart. Res. 12, 2057–2068.
- Ravel, B., Newville, M., 2005. ATHENA, ARTEMIS, HEPHAESTUS: data analysis for X-ray absorption spectroscopy using IFEFFIT. J. Synchrotron Radiat. 12, 537–541.
- Reid, G.A., Miles, C.S., Moysey, R.K., Pankhurst, K.L., Chapman, S.K., 2000. Catalysis in fumarate reductase. BBA 1459, 310–315.
- Robberecht, H., Van Grieken, R., 1982. Selenium in environmental waters: Determination, speciation and concentration levels. Talanta 29, 823–844.
- Ryser, A.L., Strawn, D.G., Marcus, M.A., Johnson-Maynard, J.L., Gunter, M.E., Möller, G., 2005. Micro-spectroscopic investigation of selenium-bearing minerals from the Western US Phosphate Resource Area. Geochem. Trans., 6
- Seders, L.A., Fein, J.B., 2011. Proton binding of bacterial exudates determined through potentiometric titrations. Chem. Geol. 285, 115–123.
- Segre, C.U., Leyarovska, N.E., Chapman, L.D., Lavender, W.M., Plag, P.W., King, A.S., Kropf, A.J., Bunker, B.A., Kemner, K.M., Dutta, P., Duran, R.S., Kaduk, J., 2000. The MRCAT insertion device beamline at the Advanced Photon Source. In: Synchrotron Radiation Instrumentation: Eleventh U.S. National Conference (ed. P. Pianetta). The 11th US national synchrotron radiation instrumentation conference (SRI99). American Institute of Physics, New York, pp. 419–422.
- Song, D., Li, X., Cheng, Y., Xiao, X., Lu, Z., Wang, Y., Wang, F., 2017. Aerobic biogenesis of selenium nanoparticles by Enterobacter cloacae Z0206 as a consequence of fumarate reductase mediated selenite reduction. Sci. Rep. 7, 3239.
- Steudel, R., Laitinen, R., 1982. Cyclic selenium sulfides. Top. Curr. Chem. 102, 177-
- Stolz, J.F., Basu, P., Santini, J.M., Oremland, R.S., 2006. Arsenic and selenium in microbial metabolism. Annu. Rev. Microbiol. 60, 107–130.
- Sustmann, R., Sicking, W., Schulz, G.E., 1989. The Active Site of Glutathione Reductase: An Example of Near Transition-State Structures. Angew. Chem., Int. Ed. Engl. 28, 1023–1025.
- Vogel, M., Fischer, S., Maffert, A., Hübner, R., Scheinost, A.C., Franzen, C., Steudtner, R., 2018. Biotransformation and detoxification of selenite by microbial biogenesis of selenium-sulfur nanoparticles. J. Hazard. Mater. 344, 749–757.
- Wang, Y., Shu, X., Hou, J., Lu, W., Zhao, W., Huang, S., Wu, L., 2018. Selenium Nanoparticle Synthesized by Proteus mirabilis YC801: An Efficacious Pathway for Selenite Biotransformation and Detoxification. Int. J. Mol. Sci., 19
- Winkel, L.H.E., Johnson, C.A., Lenz, M., Grundl, T., Leupin, O.X., Amini, M., Charlet, L., 2012. Environmental selenium research: from microscopic processes to global understanding. Environ. Sci. Technol. 46, 571–579.

Wyckoff, R.W.G., 1963. Crystal Structures. Interscience Publishers.

- Yu, Q., Boyanov, M.I., Liu, J., Kemner, K.M., Fein, J.B., 2018. Adsorption of Selenite onto Bacillus subtilis: The Overlooked Role of Cell Envelope Sulfhydryl Sites in the Microbial Conversion of Se(IV) ed. Argonne National Lab. Environ. Sci. Technol. 52, 10400–10407.
- Yu, Q., Fein, J.B., 2016. Sulfhydryl Binding Sites within Bacterial Extracellular Polymeric Substances. Environ. Sci. Technol. 50, 5498–5505.
- Yu, Q., Fein, J.B., 2017. Controls on Bacterial Cell Envelope Sulfhydryl Site Concentrations: The Effect of Glucose Concentration During Growth. Environ. Sci. Technol. 51, 7395–7402.
- Yu, Q., Szymanowski, J., Myneni, S.C.B., Fein, J.B., 2014. Characterization of sulfhydryl sites within bacterial cell envelopes using selective site-blocking and potentiometric titrations. Chem. Geol. 373, 50–58.